

## Article

# Harnessing Deep Learning for Enhanced MPPT in Solar PV Systems: An LSTM Approach Using Real-World Data

Bappa Roy <sup>1</sup>, Shuma Adhikari <sup>1</sup>, Subir Datta <sup>2,\*</sup>, Kharibam Jilenkumari Devi <sup>3</sup>, Aribam Deleena Devi <sup>4</sup> and Taha Selim Ustun <sup>5,\*</sup>

<sup>1</sup> Electrical Engineering Department, National Institute of Technology Manipur, Imphal 795004, Manipur, India

<sup>2</sup> Electrical Engineering Department, Mizoram University, Aizawl 796004, Mizoram, India

<sup>3</sup> Electronics Engineering Department, National Institute of Technology Manipur, Imphal 795004, Manipur, India

<sup>4</sup> Electrical Engineering Department, National Institute of Technology Silchar, Silchar 788010, Assam, India

<sup>5</sup> Fukushima Renewable Energy Institute, Koriyama 963-0298, Japan

\* Correspondence: mzut168@mzu.edu.in (S.D.); selim.ustun@aist.go.jp (T.S.U.)

**Abstract:** Maximum Power Point Tracking (MPPT) is essential for maximizing the efficiency of solar photovoltaic (PV) systems. While numerous MPPT methods exist, practical implementations often lean towards conventional techniques due to their simplicity. However, these traditional methods can struggle with rapid fluctuations in solar irradiance and temperature. This paper introduces a novel deep learning-based MPPT algorithm that leverages a Long Short-Term Memory (LSTM) deep neural network (DNN) to effectively track maximum power from solar PV panels, utilizing real-world data. The simulations of three algorithms—Perturb and Observe (P&O), Artificial Neural Network (ANN), and the proposed LSTM-based MPPT—were conducted using MATLAB (2021b) and RT\_LAB (24.3.3) with an OPAL-RT simulator for real-time analysis. The data used for this study were sourced from NASA/POWER's Native Resolution Daily Data of solar irradiation and temperature specific to Imphal, Manipur, India. The obtained results demonstrate that the LSTM-based MPPT system achieves a superior power tracking accuracy under changing solar conditions, producing an average output of 74 W. In comparison, the ANN and P&O methods yield average outputs of 57 W and 62 W, respectively. This significant improvement, i.e., 20–30%, underscores the effectiveness of the LSTM technique in enhancing the power output of solar PV systems. By incorporating real-world data, valuable insights into solar power generation specific to the selected location are provided. Furthermore, the outputs of the model were verified through real-time simulations using the OPAL-RT simulator OP4510, showcasing the practical applicability of this approach in real-world scenarios.

**Keywords:** maximum power point tracking; long short-term memory network; photovoltaic system; OPAL-RT simulator



**Citation:** Roy, B.; Adhikari, S.; Datta, S.; Devi, K.J.; Devi, A.D.; Ustun, T.S. Harnessing Deep Learning for Enhanced MPPT in Solar PV Systems: An LSTM Approach Using Real-World Data. *Electricity* **2024**, *5*, 843–860. <https://doi.org/10.3390/electricity5040042>

Academic Editor: Andreas Sumper

Received: 27 September 2024

Revised: 25 October 2024

Accepted: 2 November 2024

Published: 4 November 2024



**Copyright:** © 2024 by the authors. Licensee MDPI, Basel, Switzerland. This article is an open access article distributed under the terms and conditions of the Creative Commons Attribution (CC BY) license (<https://creativecommons.org/licenses/by/4.0/>).

## 1. Introduction

Today, almost every country in the world is showing great interest in the growth of renewable power because of the growing load demand for power and the lack of fossil fuels in the coming future [1]. Considered a clean resource of energy and having low maintenance requirements, photovoltaic (PV) energy is becoming significantly popular among renewable energy alternatives. However, the high cost of PV panels, low efficiency and performance deterioration over time are some drawbacks of PV [2]. The efficiency of the solar PV module in converting electric power from solar irradiation is generally less than 17%, and the generation of power depends hugely on the weather condition of the place where the PV panel is installed [3]. A maximum power point tracking (MPPT) system is applied in solar PV to take out the maximum power from the PV panel in any weather condition [4]. Tracking maximum power in solar PV mainly relies on two input parameters,

namely environmental inputs (irradiation & temperature) and electrical inputs (voltage and current).

In order to reach the maximum power point (MPP), numerous algorithm-based MPPT approaches have already been developed. Among the various traditional MPPT strategies, Perturbation and Observation (P&O) and Incremental Conductance (IC) are the most popular techniques due to their simplicity and ease of application [5,6]. As outlined by Ratnakar [7], numerous intelligence and optimisation methods are used in addition to some classical techniques, such as an Artificial Neural Network (ANN), a sliding mode controller, a fuzzy logic controller, an MPPT based on the Fibonacci series, a technique based on Gauss–Newton, ant colony optimisation, Grey wolf optimisation, artificial bee colony optimisation, and cuckoo search. In [8], a PV MPPT system is proposed for a PV water pumping system to increase its efficiency. Based on ANN, a nonlinear autoregressive moving average controller is applied to optimise the duty ratio under any irradiation condition. However, the studied model is tested with the proposed MPPT system only on a step change irradiation condition. It has been claimed that the proposed controller is better during performance and rapid in providing a response compared to a classical PID controller. An MPPT technique is proposed in [9] that is based on fuzzy logic and the P&O method. The fuzzy logic rules are adopted from a modified P&O approach for the suggested MPPT system. In [10], a sliding mode control-based MPPT is proposed, where open circuit voltage technique is used to track maximum power. By changing the duty cycle, sliding mode control tracks the maximum power. However, the projected MPPT system is not tested with varying solar irradiances and temperatures. In [11], the authors proposed an improved Fibonacci search algorithm for the MPPT system consisting of a photovoltaic array under uniform illumination conditions. Here, in this technique, the voltage analysis method is adopted for the parallel array, and a current analysis method is adopted for the series array. No real dataset or varying weather conditions are included in this research work to verify the MPPT. The PV system normally operates under different weather conditions and disturbances. Thus, there are so many unpredictable challenges that a MPPT system faces in the real world. In [12], a brand new Newton-based stochastic extreme searching MPPT method is suggested to overcome some common problems relating to existing extreme seeking controllers, such as the fact that the orthogonal requirements make it difficult for periodic extreme seeking to include situations with many variables and the fact that the control system is highly influenced by unpredictable and unknown weather (environmental) conditions. However, all these works did not concentrate further on the steady state oscillation after it reached the maximum power point. To reduce the steady state oscillation after reaching MPP, a modified particle swarm optimisation-based MPPT is proposed for photovoltaic systems [13]. The proposed method in this study was also performed under partial shading conditions. However, the variable solar irradiance and temperature are not considered, depending much on real-world conditions. Only a large step change under uniform solar irradiation and variation in load with the partial shading condition has been considered. In [14], a grey wolf optimisation-based MPPT is proposed for solar photovoltaic systems, which includes a single-ended primary-inductor converter. These techniques employ online measurements to calculate the actual MPP, and thus dirt does not influence the performance tracking. This is one of their key advantages. Still, the changes in irradiation that have been considered in order to perform the proposed method are more stable and predictable. A new MPPT controller is proposed in [15] for solar photovoltaic systems with partial shading conditions, which is based on the ant colony optimisation technique. In terms of speed of tracking, stability, accuracy, and robustness, it provides a better performance compared to other conventional techniques. Every method has its own advantages, but these also come with some disadvantages. The technique proposed in this study is so much more complex in terms of operation and is costlier. To make the photovoltaic MPPT system much simpler, a drone squadron-based algorithm is proposed in [16]. A direct control method under partial shading conditions for PV MPPT is proposed in this study. Because of the advantages, such as a fast convergence and higher

efficiency of the cuckoo search (CS) method, a CS-based maximum power point tracking system is proposed in [17]. The CS method is only capable of tracking MPP between 100–250 ms under different types of environmental change, and the performance of this method is better under steady state conditions.

When compared to other optimisation techniques, machine learning or deep learning-based solutions have a greater accuracy and degree of flexibility [18,19]. This makes them popular for various applications [20–22]. Artificial neural network-based MPPT methods are also proposed in many studies, but they face problems in terms of functioning under long-term variations of environmental conditions. To overcome these issues, a deep learning transformer-based time series prediction of MPP for solar PV is proposed in [23]. A set of environmental data is applied as input to the studied model, which is collected from 50 different locations. The levels of temperature and irradiance of different places are not the same, and only 200 consecutive hours of data are considered. Thus, the trained system for tracking the MPP of solar PV will not be able to work accurately for a particular place. Instead, if the dataset is collected from a particular area over a long period of time, the trained network will have the actual environmental idea and will be able to work more accurately with the variations in the weather conditions.

In this paper, a deep-learning Long Short-Term Memory (LSTM)-based solar PV MPPT system is proposed to extract maximum power from the PV system. The solar irradiation and temperature from Native Resolution Daily Data of NASA/POWER CERES/MERRA2, for the time range of 1 January 2017 to 31 March 2021, are considered as input parameters to obtain the system response under real input data [24]. A real set of data input for a particular location in India (Imphal, Manipur) is utilised for the solar PV system, which will provide actual weather conditions to the system. The trained LSTM network provides the reference voltage from the environmental inputs and is compared with the actual inputs to provide a pulse signal to the boost converter of the solar PV system. The proposed MPPT system is compared with P&O MPPT and ANN-based MPPT. In terms of tracking, the MPP-proposed LSTM technique provides a much better, stable, and accurate response compared to P&O MPPT and ANN-based MPPT. Real-time verification of the studied model is conducted in an RT-LAB environment with the help of the real-time simulator OP4510.

The remaining part of the paper is structured as follows. The researched model and suggested technique are introduced in Section 2, the results are analysed in Section 3, and the conclusions are drawn in Section 4.

## 2. Modelling and Methods

In this section, the studied model is discussed along with the real-time modeling steps of the studied PV system. Then, different techniques of solar PV MPPT along with the proposed MPPT technique are illustrated.

### 2.1. Modelling

Figure 1 shows the solar PV-MPPT system in use. An MPPT controller, a boost converter, a PID controller, and a pulse-width-modulation generator are the parts of the solar panel. The components that make up the system are described below [9,11].

#### 2.1.1. PV Panel

In order to generate electricity from solar irradiation, PV cells typically feature a p-n junction that is constructed in a thin layer of semiconductor ingredients. There are two different PV model types: single-diode and double-diode. Due to their simplicity, single-diode models are preferred over double-diode models, though double-diode models are more accurate. Figure 2 depicts an equivalent circuit for a PV solar cell.

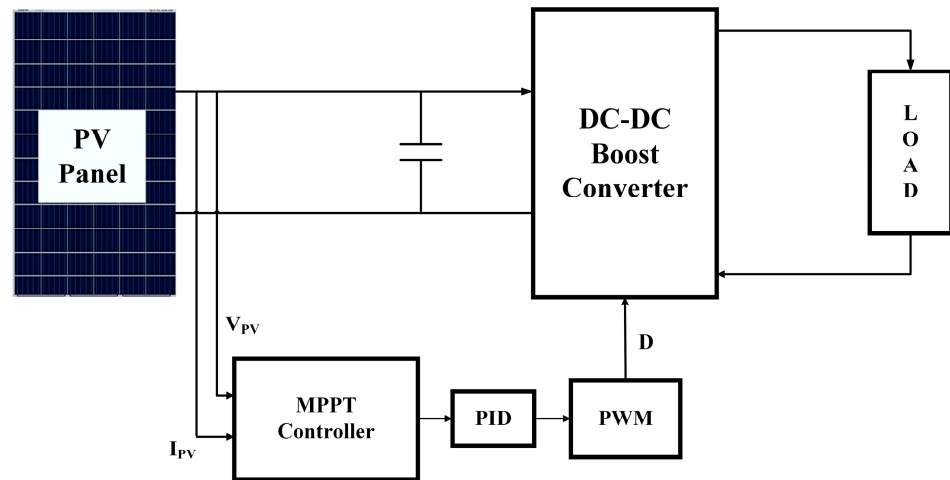


Figure 1. Solar PV-MPPT system.

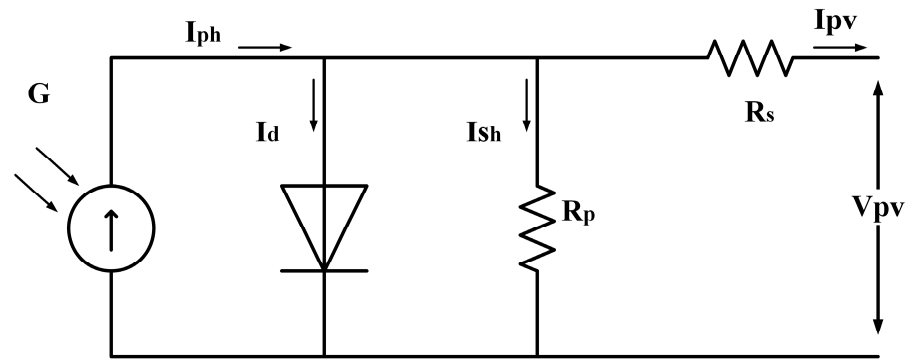


Figure 2. PV solar cell equivalent circuit.

The output current of an ideal cell based on Kirchoff’s law is given by:

$$I = I_{ph} - I_d - I_{sh} \tag{1}$$

where  $I_{sh}$  is the parallel resistance current, which is given by:

$$I_{sh} = \frac{V + IR_s}{R_p} \tag{2}$$

where  $R_p$  and  $R_s$  are the resistances in parallel and in series, respectively.

$I_{ph}$  is the light-generated current given by:

$$I_{ph} = [I_{sc} + K_1(T_c - T_r)] \times \frac{G}{G_{STC}} \tag{3}$$

where the short circuit current is denoted by  $I_{sc}$  at standard circumstance ( $T = 25$ ,  $G_{STC} = 1000 \text{ W/m}^2$ ),  $K_1$  is the temperature-related short circuit current coefficient,  $T_c$  is the temperature of the cell,  $T_r$  is the reference temperature, and the relative irradiance is denoted by  $G$ .

The diode current  $I_d$  is given by [9]:

$$I_d = I_0 \left[ \exp\left(\frac{qV_d}{AKT_c}\right) - 1 \right] \tag{4}$$

where the electrical charge  $q = 1.6 \times 10^{-19}$ , Boltzmann's constant  $K = 1.38 \times 10^{-23}$ ,  $A$  is the diode ideal factor, the reverse saturation current is denoted by  $I_0$ , and the diode equivalent voltage is denoted by  $V_d$ .  $V_d$  is calculated by [9]:

$$V_d = V + IR_s \quad (5)$$

In PV modules, PV cells are normally linked in series. The output current of a PV module actively depends on the solar irradiation and temperature, which is given by:

$$I_{pv} = I_{ph} - I_0 \left[ \exp\left(\frac{q(V + IR_s)}{AKT_c N_s}\right) - 1 \right] \quad (6)$$

where the number of series-connected cells is denoted by  $N_s$ .

The PV panel used in this work is constructed as one parallel string, one series-connected module string, and 60 cells per module. The measurements of the solar PV panel are recorded in Table 1 [11].

**Table 1.** Parameters of PV panel.

Parameters	Measurements
$V_{OC}$	37.3 V
$I_{SC}$	8.66 A
$V_{mp}$	30.7 V
$T_{coeff}$ of $V_{OC}$	-0.36901%/deg.C
$T_{coeff}$ of $I_{SC}$	0.086998%/deg.C

### 2.1.2. DC–DC Boost Converter

A boost DC–DC boost converter is extensively utilised in photovoltaic (PV) systems due to its high efficiency and compatibility with Maximum Power Point Tracking (MPPT) controllers. This converter regulates the output voltage to levels significantly higher than the input voltage. The core component of the DC–DC boost converter is a transistor, typically a MOSFET, which is regulated by a controller to manage the voltage amplification. It takes the input from the solar panel, and the output of the DC–DC boost converter is connected to the load, as shown in Figure 3. The voltage gain of the converter is defined by Equation (7) [9]:

$$G = \frac{V_0}{V_i} = \frac{1}{1 - D} \quad (7)$$

where  $V_0$  is the output voltage,  $V_i$  is the input voltage, and the duty cycle is denoted by  $D$ , controlled via the gate driver circuit.

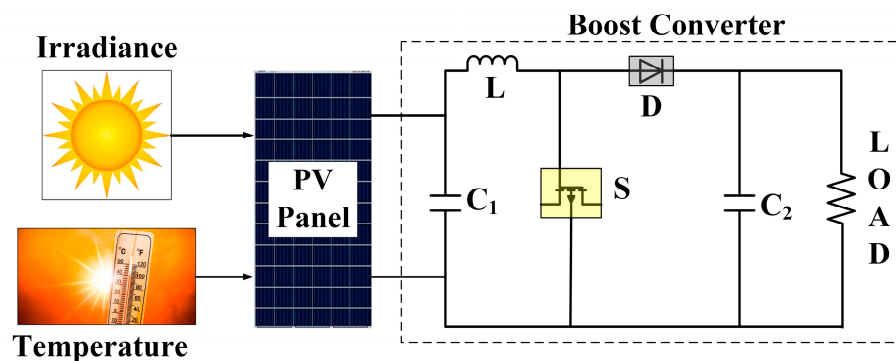


**Figure 3.** DC–DC boost converter.

The operation of the DC–DC boost converter involves two primary states:

- State 1: When the MOSFET is switched on, current flows through the inductor (L) in the reverse direction, causing it to store energy in the form of a magnetic field. During this state, the output capacitor (C2) supplies energy to the load or inverter.
- State 2: When the MOSFET is switched off, the stored energy in the inductor combines with the input source, resulting in a higher output voltage.
- This dual-state operation ensures efficient energy conversion and voltage regulation, making the DC–DC boost converter a vital component in PV systems.

### 2.1.3. PID Controller

With the aim of causing the PV system to operate at its optimum productivity, a PID controller is connected to the anticipated voltage. A Proportional-Integral-Derivative (PID) controller is a crucial feedback mechanism widely used in PV systems for Maximum Power Point Tracking (MPPT). It enhances system performance by minimising the error between the desired and actual outputs, thus ensuring optimal energy harvest.

The PID controller comprises three components: Proportional Control (P), Integral Control (I), and Derivative Control (D). Proportional Control reacts to the instantaneous error, thereby enhancing system responsiveness but potentially causing overshoot. Integral Control accounts for the cumulative sum of past errors, effectively eliminating steady-state error, though it may slow the system response. Derivative Control responds to the rate of change of the error, thereby improving system stability and reducing the likelihood of overshoot.

### 2.1.4. Real-Time Modelling

For the real-time simulation of any MATLAB model, models need to be designed for the RT-lab interface. The RT-lab interface supports the subsystem of the MATLAB/Simulink developed model. The MATLAB/Simulink (2021b) model needs to be designed as several subsystems, a minimum of two subsystems, namely SM\_subsystem2 and SC\_subsystem1. Depending on the complexity of the subsystem, the model can be divided into more than two subsystems. However, the number of maximum subsystems depends on the core of the OPAL-RT simulator. SC\_subsystem1 is the output part of the model where the result will be displayed. All the inputs coming to this subsystem will be connected through an OPCOMM block, and the computational part of the model cannot be placed here.

SM\_subsystem2 is the part of the model where all the computational things of the model will be placed. If, depending on the complexity of the model, the number of subsystems becomes more than two, then those subsystems will be named SS\_subsystem3, SS\_subsystem4. In real-time modelling, the naming of the subsystems plays a critical role. Without properly naming the subsystems, we will be unable to add OPCOMM to the model design in the Simulink environment, which is a mandatory component of real-time modelling. The naming of subsystems must follow the sequence, as discussed above. The OPCOMM block functions as a communicated system between the Host and Target simulator.

The studied system is considered for real-time simulation with the help of MATLAB and RT-lab. The developed model of the studied solar system is shown in Figure 4. The OPAL-RT simulator OP4510 is connected to the host PC through an ethernet cable. The PC contains both MATLAB and RT-LAB, referred to as the host system. A Simulink model must successfully run in MATLAB before it can be executed in RT-lab. The RT-lab interface allows us to open Simulink models, and if the model is properly designed for real-time simulation, we can execute it by following the RT-lab execution steps.

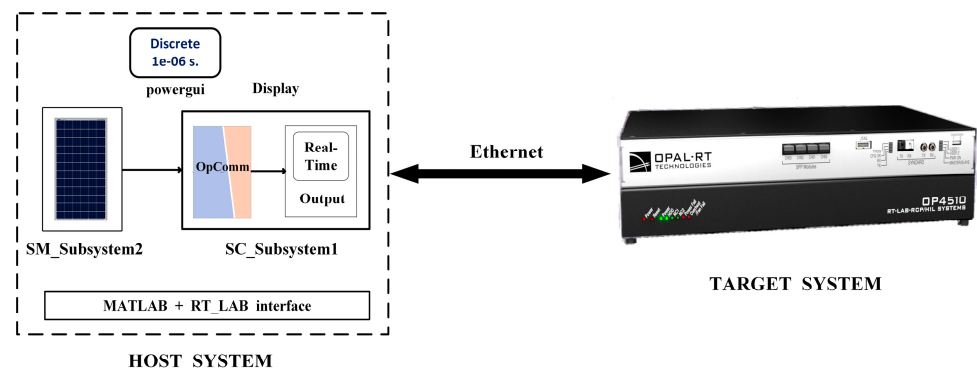


**Figure 4.** Real-time operation.

## 2.2. Data Collection

The effectiveness of a solar panel decides various factors related to weather conditions and solar irradiation and temperature. Also, parameters of the location where PV panels are installed play a critical part in determining the MPP. Thus, solar irradiation and temperature are utilised as input in this work. The data have been collected for the city of Imphal in India from 1 January 2017 to 31 March 2021, from Native Resolution Daily Data of NASA/POWER CERES/MERRA2. This dataset of irradiation and temperature is shown in Figure 5 as the signal response form. Using this daily dataset, one can understand the real weather conditions that make the model more realistic and effective.

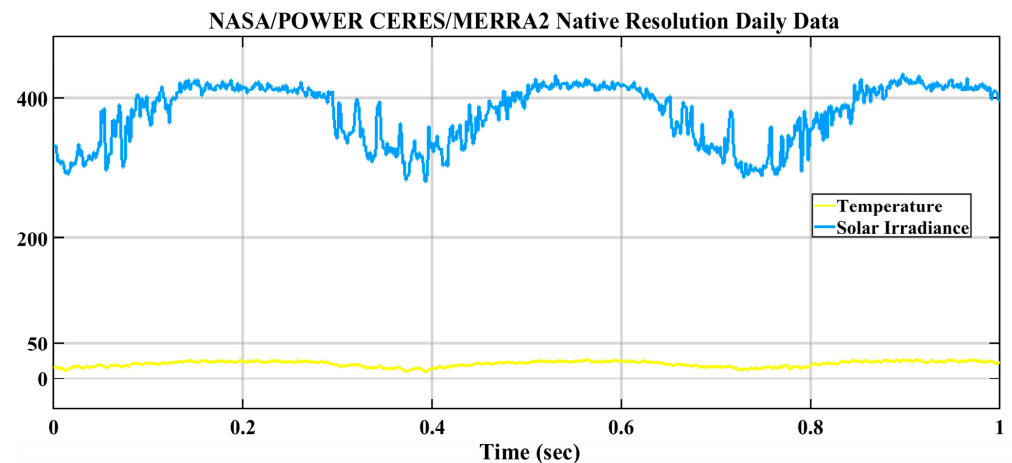


**Figure 5.** Native resolution daily data of NASA/POWER CERES/MERRA2 (Imphal, India).

## 2.3. Methods

In this section, different MPPT techniques are illustrated along with the proposed MPPT techniques.

### 2.3.1. P&O MPPT

A popular solution for solar PV MPPT is P&O-based, since it is simple to construct and has a straightforward functionality. By altering the PV voltage level or the boost converter's duty cycle, the maximum power point is controlled using the voltage of the PV panel as an input. Figure 6 depicts a flow diagram of the P&O approach, where "K" represents the voltage or current of the solar PV module [5].

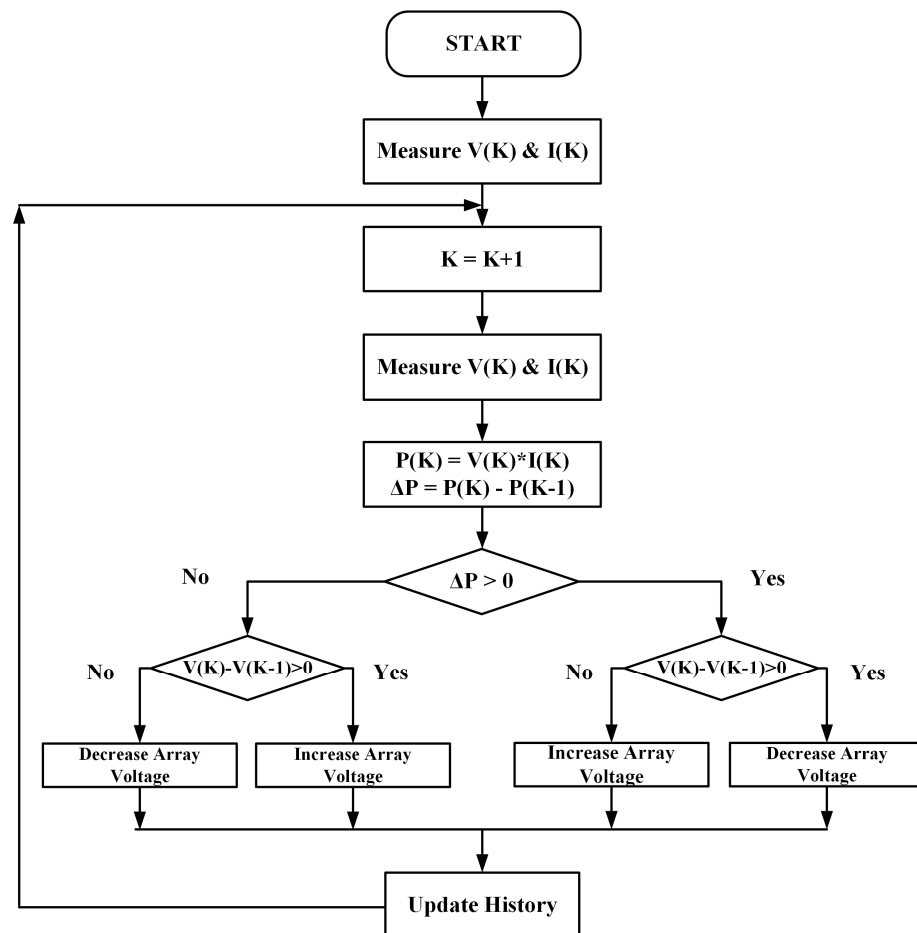


**Figure 6.** Flowchart of P&O algorithm.

The direction of the next perturbation will change to move the operating power to the MPP if altering the PV module's voltage or current or the boost converter's duty cycle results in an increase in power output.

### 2.3.2. Artificial Neural Network MPPT

The ANN is a summation of several organised neurons, the same as the human brain. Adjustable weights connect one neuron with another, and signals pass through it. The learning process of weights is conducted by frequently changing their values. A collection of input (predictions) and output (targets) values are necessary for training the network. Every neuron calculates the activation level of the signals that are connected to it. Error is calculated after each iteration by comparing the output and input values. This process is repetitive until the error value reaches the desired value [1]. The Simulink model of the ANN-based method is shown in Figure 7. The Function Fitting Neural Network contains the trained ANN model, which is developed and trained using MATLAB's function fitting toolbox. This trained network receives solar irradiance and temperature as inputs. The reference voltage is compared with the actual voltage, and it is processed through a PID controller before being applied to PWM.

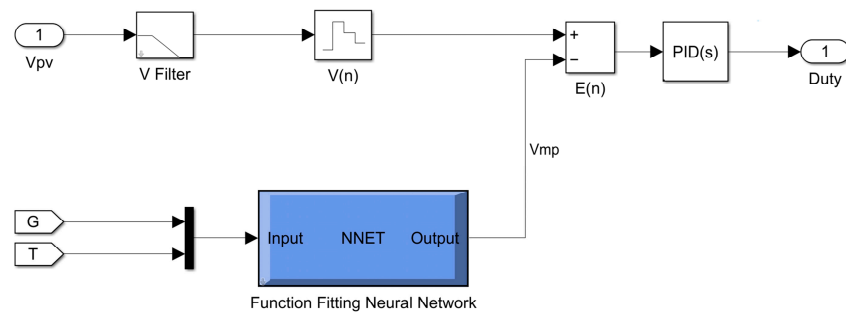


Figure 7. Simulink model for ANN method.

2.3.3. Deep LSTM MPPT

The P&O method is a straightforward and simple technique commonly used for MPPT. In this method, a daily dataset of irradiation and temperature is provided as input to the system. The current and voltage of the PV panel are used as input signals for the MPPT system. In the neural network, MPPT technique Native Resolution Daily Data of NASA/POWER CERES/MERRA2 of solar irradiation and temperature is given as input to the main system, and the same set of data is also used as input to the deep LSTM MPPT [24]. The detailed architecture and working principle are discussed by Kah Yung Yap et al. [25]. The LSTM algorithm is taken into consideration for the creation of a deep learning-based solar MPPT due to its many advantages over other networks. Hochreiter & Schmidhuber first introduced the LSTM network in 1997, which is a more sophisticated RNN type. This method has been utilised for power system load forecasting [26], LSTM is used for rapid detection in power systems [27], and numerous additional studies [28] have demonstrated that LSTM is becoming more and more popular in the field of power systems because of its capacity for multitasking learning. In order to provide long-term information storage and access, a memory cell is introduced into the RNN framework and runs down the entire chain. The LSTM uses various auxiliary gates to add info to the memory cell. Any entries from the cell are subject to output gate control. The input gate determines when the data must be read, and the forget gate performs the cell's reset. Figure 8 illustrates a fundamental LSTM construction that is provided in the literature.

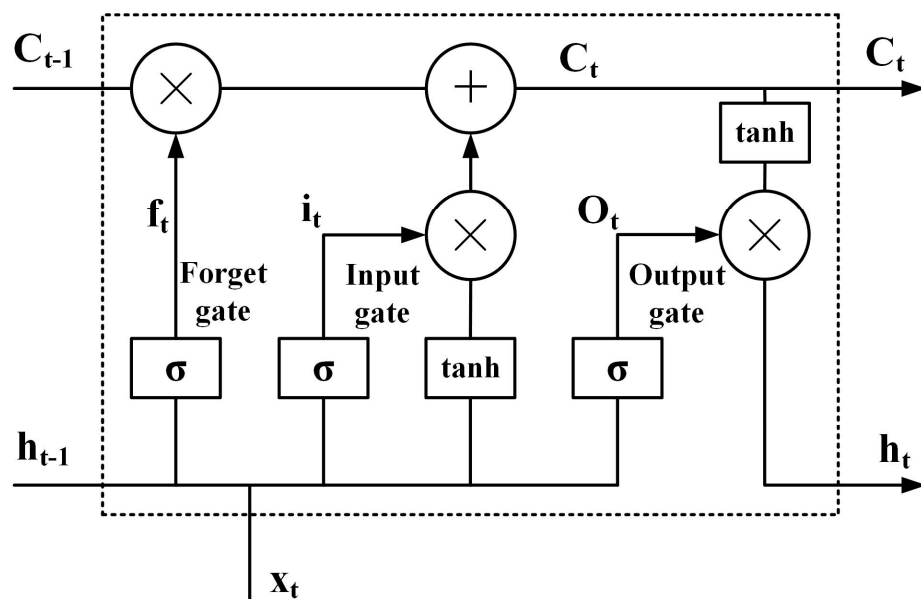


Figure 8. The LSTM cell structure.

Here, the LSTM unit's current output and current state quantity, respectively, are denoted by  $h$  and  $c$ .

The control formula of the LSTM is as follows:

$$\begin{aligned}
 f_t &= \sigma(W_{fx}x_t + W_{fh}h_{t-1} + b_f), \\
 i_t &= \sigma(W_{ix}x_t + W_{ih}h_{t-1} + b_i), \\
 g_t &= \phi(W_{gx}x_t + W_{gh}h_{t-1} + b_g), \\
 c_t &= f_t \odot c_{t-1} + i_t \odot g_t, \\
 o_t &= \sigma(W_{ox}x_t + W_{oh}h_{t-1} + b_o), \\
 h_t &= o_t \odot \phi(c_t).
 \end{aligned} \tag{8}$$

where  $i_t$ ,  $f_t$ , and  $o_t$  are the input gate, forget gate, and output gate, respectively,  $W_{fx}$ ,  $W_{fh}$ ,  $W_{ix}$ ,  $W_{ih}$ ,  $W_{ox}$  and  $W_{oh}$  are the weight parameters of the network activation function, and  $b_f$ ,  $b_i$  and  $b_o$  are the offset vectors.  $\phi$  is the sigmoid activation function,  $g_t$  is the candidate memory cell, whose weight parameters are  $W_{gx}$  and  $W_{gh}$ , and  $b_g$  is the offset vector. Computation is similar to the three gates but uses  $\phi$  as a tanh activation function.  $C_t$  is the memory cell and is the multiplication of the Hadamard product matrix.  $C_t$  merges the information of the current candidate memory cell and previous time-step memory cell to control the flow of information. The hidden state is denoted by  $h_t$ . The flow of information through the output gate, from the memory cell to the hidden state, can be controlled, where  $\phi$  ensures the value range of the hidden state.

This technique aims to trace the maximum power from a real dataset of temperature and solar irradiance in order to maximise power production. This technique is based on the LSTM deep-learning model. The proposed approach has three main steps, which are the collection of historical data from the PV system, filtering and normalising the data, and lastly training, validating and testing the LSTM model. A block chart of the LSTM tracking approach is given in Figure 9.

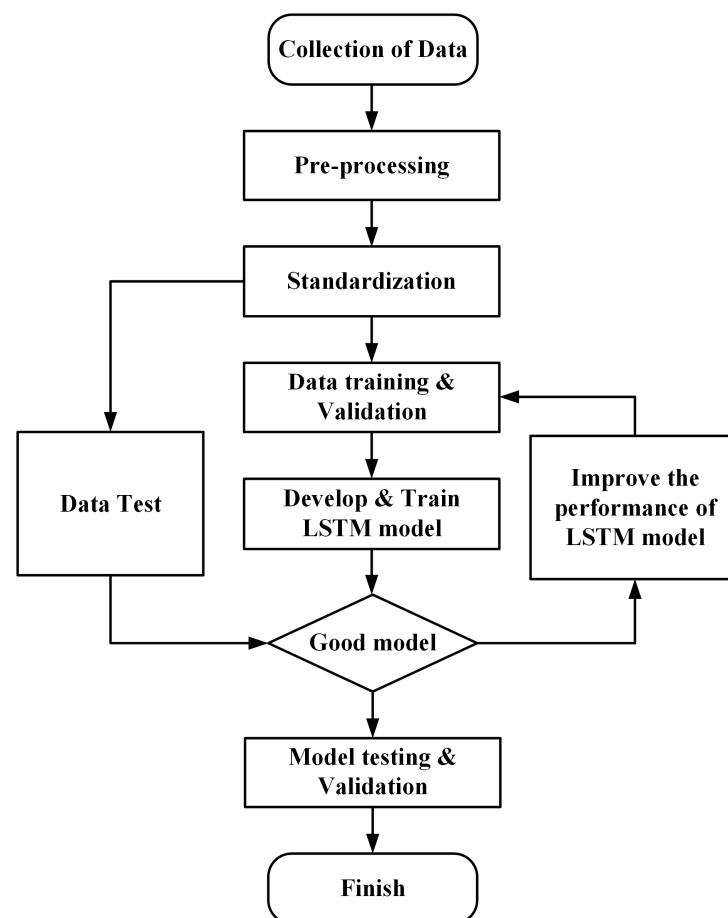


Figure 9. Flowchart for LSTM.

The developed LSTM network is shown in Figure 10 as a Simulink diagram. This model is developed with the help of MATLAB/Simulink. The ‘Stateful Predict’ block in Simulink is used to contain the trained LSTM network. It receives the same input signals as the P&O and ANN models.

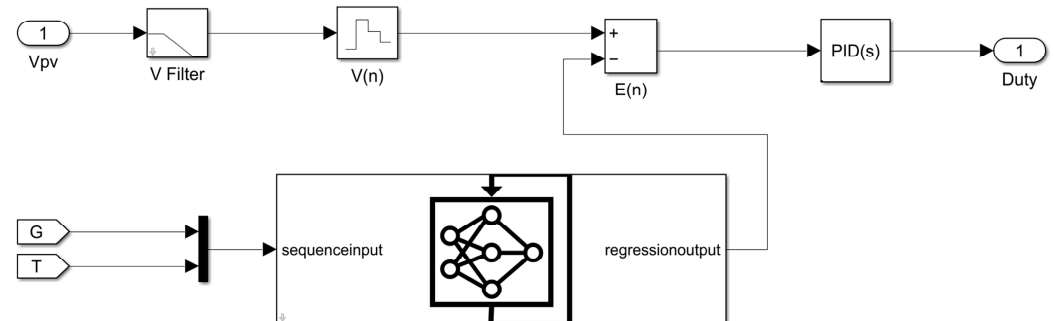


Figure 10. Simulink model of deep LSTM.

Ten thousand historical input and output data points are used for the LSTM network’s training, and thirty percent of those data points are used for testing. A total of 200 hidden units have been spread throughout a total of four layers. LSTM, sequence input, fully connected, and regression layer make up the layers. There are 250 training epochs. The model constraint values are listed in Table 2.

Table 2. LSTM model constraints.

Hidden Units	Optimiser	Initial Learning Rate	Drop Factor	Max Epochs
200	adam	0.005	0.2	250

### 3. Results and Discussion

The studied model for the proposed work is designed and analysed in the MATLAB/Simulink environment. A performance outcome is gathered, such as voltage, current, and solar power. The suggested Deep LSTM-based approach performance is compared with existing techniques of P&O and artificial neural networks. Solar PV power is the product of solar PV voltage and solar PV current. A solar PV module will produce its maximum current in the absence of any resistance in the circuit. The solar PV module is called shorted when the voltage in the circuit is zero. Figure 11 shows the proposed Simulink design of the solar PV system. The studied model receives real-world data from the ‘From Spreadsheet’ block in Simulink as input. A DC–DC boost converter is connected to a user-defined PV panel, controlled by the MPPT signal. The MPPT controller is alternately replaced with P&O, ANN, and LSTM techniques, and the model is simulated for each. The output results are analysed and compared.

A real-world-based solar irradiation and temperature data signal is used, as shown in Figure 5, for the simulation of the model. Figure 12a presents the power outputs, Figure 12b shows voltage outputs, and Figure 12c illustrates the simulation current outputs for all three MPPT techniques, P&O, ANN, and LSTM.

The MPPT system is used in the studied model under a real-world dataset to predict the reference voltage under real-life solar irradiation and temperature conditions. As shown in Figure 5, the solar irradiance and temperature change rapidly. Thus, by considering the real dataset, the studied model does not need to be tested under different weather conditions, such as partial shading, step change in input, etc. The studied model is simulated under real-world conditions by considering a real set of data, and the model is verified for real-time simulation by applying a real-time simulator in the OPAL-RT/Simulink environment. Figure 13 shows the OPALRT setup for real-time validation.

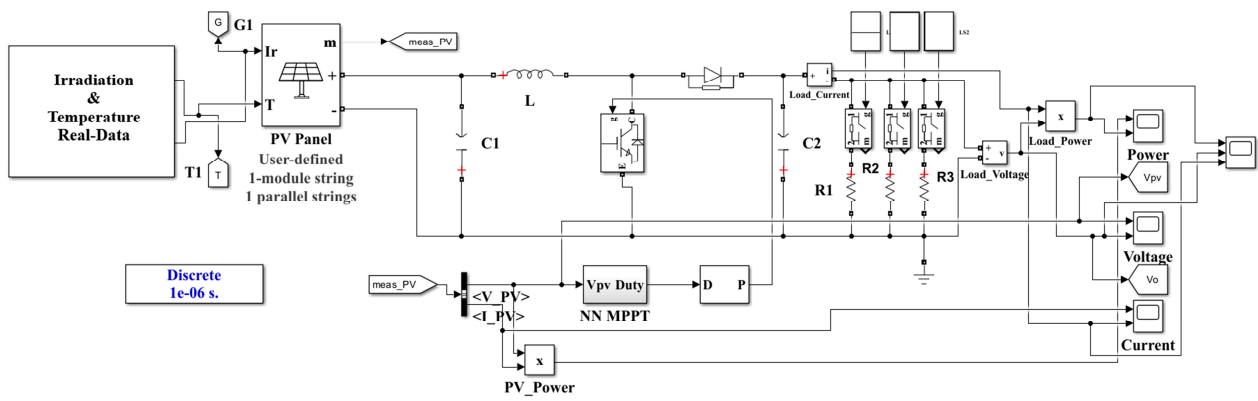
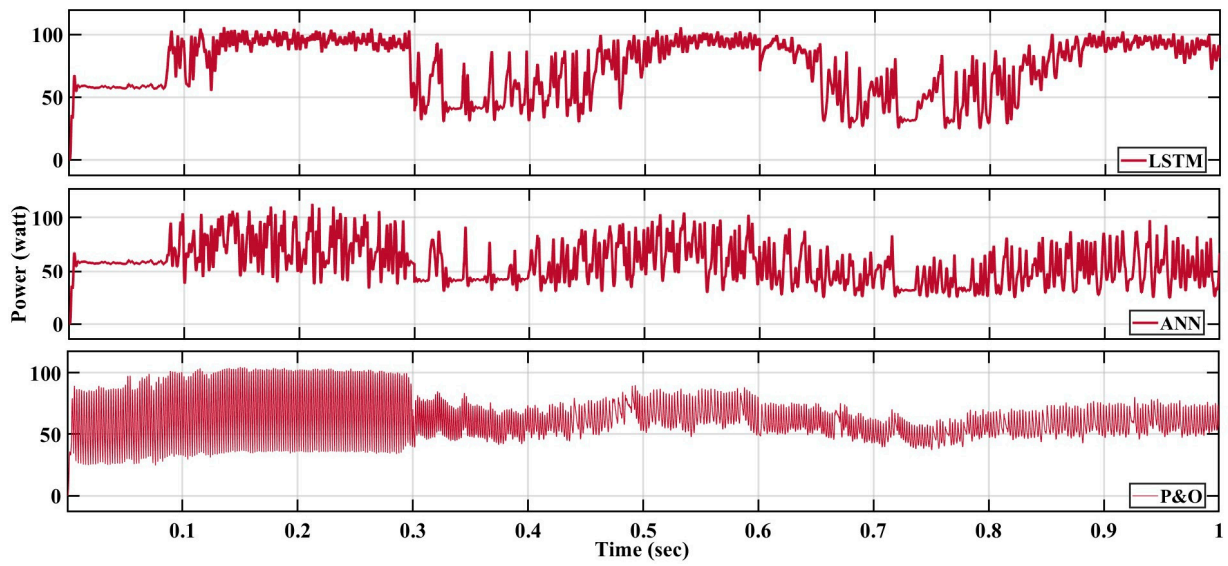
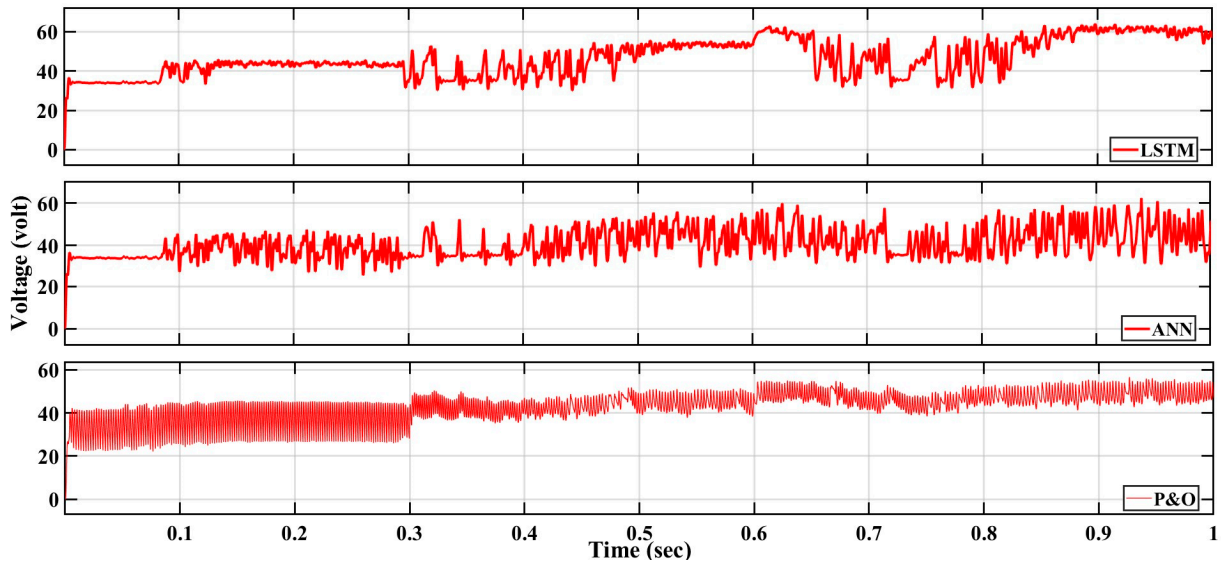


Figure 11. The studied MATLAB/Simulink model with real dataset.



(a)



(b)

Figure 12. Cont.

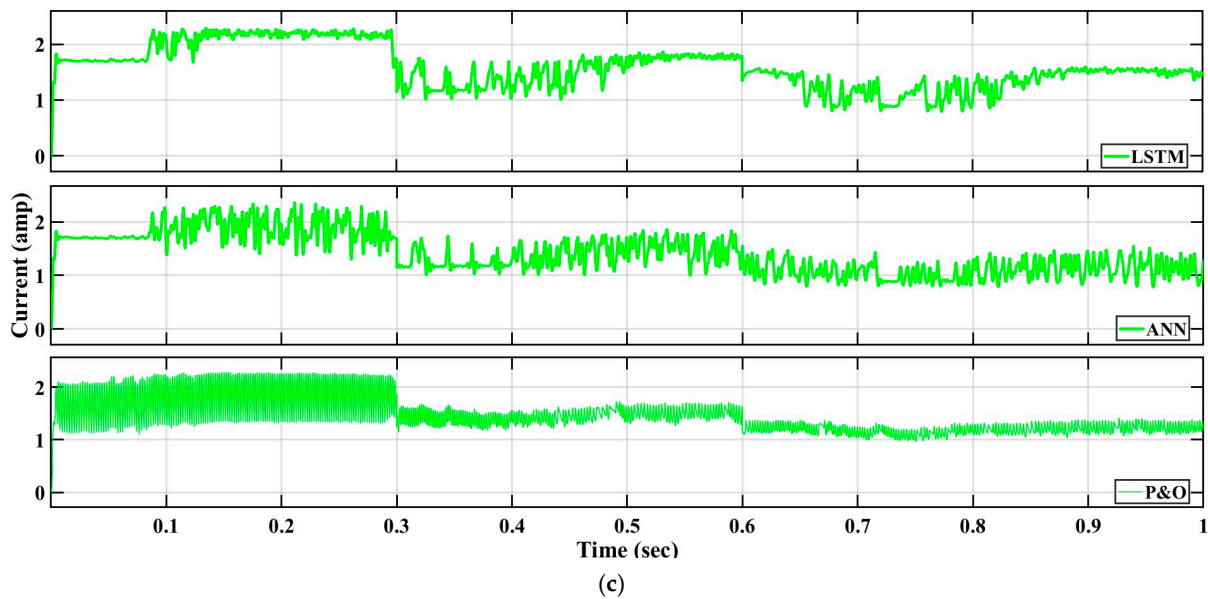


Figure 12. Comparison of (a) power, (b) voltage, and (c) current outputs under real-world data.



Figure 13. OPALRT setup for real-time validation.

Figure 12a shows that there is so much variation in power output for the P&O-based MPPT technique of solar PV systems. Thus, from the power output signal of Figure 12a, it is clear that the P&O technique is able to track the MPP, but not so well enough with rapidly changing inputs. Also, the voltage and current response of the P&O-based technique, as illustrated in Figure 12b,c, varies continuously with varying input.

The variation in the power output, depending on the varying inputs of the solar PV system, can also be seen in the ANN-based MPPT method in Figure 12a. The power output signal of Figure 12a shows that under rapidly changing conditions of inputs, ANN can track the MPP but that there are still so many variations present in the tracking process. The variations are also present in the voltage and current signal of ANN-based MPPT, as shown in Figure 12b,c, respectively.

The proposed deep LSTM technique-based simulation power output is also displayed in Figure 12a for a better comparison. The output power, as well as the voltage and the current output signal, gives a more stable response under varying real-world datasets of inputs (irradiation and temperature), as shown in Figure 12a–c, respectively. This stable output of power shows so much less oscillation, and for the safety of the equipment

connected to the solar system, a stable output is very much needed. As a result, the LSTM-based technique is the most accurate and effective in tracking the MPP.

When comparing the LSTM approach with existing techniques such as P&O and ANN, its superior performance stems from its ability to handle sequential and time-series data more effectively. LSTM networks are designed to retain and update information over time, allowing them to capture temporal dependencies better than P&O, which makes iterative adjustments, or ANN, which lacks memory capabilities. This enables LSTM to learn from dynamic patterns in solar irradiance and temperature, leading to more accurate MPPT predictions and improved stability under varying conditions, making it well-suited for real-world solar PV systems.

A detailed comparison of the power output of the proposed LSTM technique with two existing techniques is provided in Table 3. The time durations for the comparison are considered depending on the output results. Table 4 presents a comparison among these three MPPT techniques with quantitative data, with three distinct sets of numerical output power data generated by implementing three different MPPT techniques (denoted as LSTM, ANN, and P&O) within a PV model. It is noteworthy that the input parameters remained consistent across all three cases, ensuring comparability of results. To enhance the robustness of the analysis and mitigate the influence of noise inherent in the data, each output dataset was partitioned into ten distinct segments, as shown in Table 4. Subsequently, the average power output values were calculated for each of these segments within each dataset. By aggregating these segment-wise averages, we obtained three unique average values representing the overall performance of each MPPT technique. Notably, the observed disparity in average power outputs underscores the superior performance of the LSTM technique, which yielded an average output of 74 W, compared to the ANN and P&O techniques, which yielded averages of 57 and 62 W, respectively.

**Table 3.** Comparison of LSTM-, P&O- and ANN-based MPPT.

Time (s)	P&O-Based MPPT	ANN-Based MPPT	LSTM-Based MPPT
(0–0.1) s	The power output oscillates so much throughout this time period, demonstrating that this technique is unable to measure MPP accurately under input changes that are quick.	Oscillation in the power output is not present, and it is able to track MPP with more accuracy.	Oscillation in the power output is the same as for the ANN-based technique, but better compared to the P&O technique. It can track the MPP with accuracy.
(0.1–0.3) s	Here, in this time duration, oscillation in the power output is higher and unpredictable compared to the ANN and LSTM technique. To track the MPP, this technique faces inaccuracy compared to other techniques.	Oscillation in power output is less compared to the P&O technique, but more compared to the LSTM technique.	Compared to both the P&O- and ANN-based techniques, the LSTM-based technique provides a significantly greater response throughout this time period and is able to more accurately track MPP.
(0.3–0.5) s	Depending on the input's oscillation, it is less in this time duration.	Oscillation in power output is less compared to the P&O technique, but the same as for the LSTM technique.	In this time duration, oscillation in the power output is less compared to the P&O technique but the same as for the ANN technique.
(0.5–0.65) s	Oscillation in the power output is higher compared to the ANN and LSTM techniques.	Here, in this time duration, oscillation in the power output is less compared to the P&O method, but more compared to the LSTM method.	Oscillation in the power output is less compared to both P&O and ANN techniques, tracking MPP with more accuracy and giving a stable power output.
(0.65–0.85) s	In this time duration, the P&O-based technique provides a power output full of oscillation present in it depending on the changes in the inputs.	The power output response is almost the same as for the LSTM-based technique, but less compared to the P&O method.	The power output response is almost the same as for the ANN-based technique, but less compared to the P&O method.

Table 3. Cont.

Time (s)	P&O-Based MPPT	ANN-Based MPPT	LSTM-Based MPPT
(0.85–1) s	The average oscillation in the power output is less compared to the ANN method, but more compared to the LSTM method.	Oscillation is higher compared to both P&O and LSTM methods.	Oscillation is less compared to both P&O and ANN methods.

Table 4. Quantitative comparison of LSTM-, P&amp;O- and ANN-based MPPT.

SL No.	Simulation Time (s)	Data Range		LSTM	ANN	P&O
1	0.05 to 0.1 *	50,000 to 100,000	Min	56.486	40.912	24.505
			Max	103.073	110.342	101.362
			Avg	66.920	62.746	63.794
2	0.1 to 0.2	100,001 To 200,000	Min	54.910	37.614	29.333
			Max	105.897	110.342	104.600
			Avg	91.757	75.534	70.163
3	0.2 to 0.3	200,001 To 300,000	Min	49.161	33.108	33.841
			Max	104.810	112.843	103.297
			Avg	93.472	69.719	70.594
4	0.3 to 0.4	300,001 To 400,000	Min	30.215	30.278	39.173
			Max	93.494	91.602	84.790
			Avg	51.127	46.290	59.386
5	0.4 to 0.5	400,001 To 500,000	Min	29.869	30.091	44.216
			Max	99.689	94.893	89.820
			Avg	66.749	59.886	63.542
6	0.5 to 0.6	500,001 To 600,000	Min	73.709	29.155	47.663
			Max	105.826	104.790	88.119
			Avg	93.527	68.396	67.965
7	0.6 to 0.7	600,001 To 700,000	Min	25.105	24.605	42.676
			Max	99.541	90.101	75.691
			Avg	68.822	49.381	58.678
8	0.7 to 0.8	700,001 To 800,000	Min	24.448	24.816	37.028
			Max	83.624	83.511	70.298
			Avg	46.935	39.902	51.370
9	0.8 to 0.9	800,001 To 900,000	Min	28	24.359	42.524
			Max	103	87.427	76.917
			Avg	76.46	51.842	57.832
10	0.9 to 1	900,001 To 1,000,000	Min	71.698	24.009	45.663
			Max	102	97.707	80.215
			Avg	91.625	53.875	60.528

\* 0 to 0.05 s of simulation time is not considered in this analysis for a better analysis of averages because there are null values present in this time duration.

From the analysis of the power output, it is evident that the proposed LSTM technique is a superior method for the MPPT of solar systems. This suggests that priority should be given to this technique when developing MPPT solutions for solar PV systems, as the analysis shows that it yields a higher power output compared to the other techniques evaluated.

However, the proposed technique has been tested using real-world data from a specific location. Consequently, one could question whether its superior performance is location-dependent. Nevertheless, deep-learning algorithms, such as the LSTM, have the inherent ability to learn features from the data, which may allow the technique to continuously adapt and perform well, even when the location or input data changes.

Additionally, further clarity on the performance of the suggested MPPT technique could be achieved by testing it on predicted input data over a longer time horizon for solar PV systems. This would provide a more comprehensive understanding of its potential and robustness under varying conditions.

#### 4. Conclusions

The proposed LSTM-based deep learning Maximum Power Point Tracking (MPPT) system demonstrates significant advancements in optimising solar photovoltaic (PV) power generation. Through the analysis of real-world data sourced from NASA/POWER CERES/MERRA2's Native Resolution Daily Data for solar irradiation and temperature in Imphal, Manipur, India, the effectiveness of the LSTM algorithm under dynamic conditions has been established. Comparative evaluations reveal that the LSTM technique achieves an average output of 74 W, representing an increase of approximately 29.82% over the Perturb and Observe (P&O) method, which yields an average of 57 W, and a 19.35% improvement over the Artificial Neural Network (ANN), which averages 62 W. These results underscore the superior tracking accuracy of the LSTM-based MPPT system, especially under rapidly changing environmental conditions.

The validation of the model was conducted using a solar PV system equipped with a boost converter connected to a variable load, with real-time simulations performed using the OPAL-RT simulator OP4510. This approach reinforces the practical applicability of the LSTM-based MPPT in real-world scenarios. The incorporation of real-world data not only enhances the model's reliability but also provides crucial insights into solar power generation dynamics specific to the studied location. Overall, the findings contribute to the ongoing development of more efficient MPPT strategies in solar energy systems, highlighting the potential of deep-learning techniques in this domain.

#### 5. Directions for Future Research

This research work was conducted at the location of Imphal, India, and the results indicate that the proposed MPPT technique for the solar PV system yields a higher power output compared to conventional methods. Therefore, this technique can be recommended for the design of MPPT systems for solar installations in this specific region. Furthermore, there is a potential to test the proposed LSTM technique using a longer range of future predicted input data for the location, which would enhance the reliability and robustness of the proposed method.

Future research could also focus on the scalability of the LSTM MPPT technique in larger and more complex solar PV systems, including multiple interconnected arrays. Additionally, exploring the integration of the LSTM-based MPPT method within hybrid energy systems that combine solar PV with other renewable sources, such as wind or hydroelectric power, could evaluate its effectiveness in a multi-source environment.

**Author Contributions:** Conceptualization, B.R. and S.A.; methodology, B.R., S.A., S.D. and T.S.U.; software B.R.; validation, B.R., formal analysis, S.A., S.D. and T.S.U.; investigation B.R. and S.A.; resources, K.J.D., A.D.D. and T.S.U.; writing—original draft preparation, B.R., S.A. and S.D.; writing—review and editing, B.R., K.J.D., A.D.D. and T.S.U.; visualization, S.D. and T.S.U.; supervision, S.A., S.D. and T.S.U.; project administration, S.A., K.J.D., A.D.D. and T.S.U.; Funding acquisition, T.S.U. All authors have read and agreed to the published version of the manuscript.

**Funding:** This research received no external funding.

**Data Availability Statement:** Data are contained within the article.

**Conflicts of Interest:** The authors declare no conflicts of interest.

## References

1. Latif, A.; Paul, M.; Das, D.C.; Hussain, S.M.S. Price Based Demand Response for Optimal Frequency Stabilization in ORC Solar Thermal Based Isolated Hybrid Microgrid under Salp Swarm Technique. *Electronics* **2020**, *9*, 2209. [CrossRef]
2. Ustun, T.S.; Nakamura, Y.; Hashimoto, J.; Otani, K. Performance analysis of PV panels based on different technologies after two years of outdoor exposure in Fukushima. *Jpn. Renew Energy* **2019**, *136*, 159–178. [CrossRef]
3. Chauhan, A.; Upadhyay, S.; Khan, M.T. Performance Investigation of a Solar Photovoltaic/Diesel Generator Based Hybrid System with Cycle Charging Strategy Using BBO Algorithm. *Sustainability* **2021**, *13*, 8048. [CrossRef]
4. Chander, A.H.; Rao, K.D.; Teja, B.P.; Sahu, L.K.; Dawn, S.; Alsaif, F.; Alsulamy, S. A Transformerless Photovoltaic Inverter with Dedicated MPPT for Grid Application. *IEEE Access* **2023**, *11*, 61358–61367. [CrossRef]
5. Mazumdar, D.; Biswas, P.K.; Sain, C. GAO Optimized Sliding Mode Based Reconfigurable Step Size P&O MPPT Controller with Grid Integrated EV Charging Station. *IEEE Access* **2024**, *12*, 10608–10620.
6. Shang, L.; Guo, H.; Zhu, W. An improved MPPT control strategy based on incremental conductance algorithm. *Prot. Control. Mod. Power Syst.* **2020**, *5*, 14. [CrossRef]
7. Ballipo, R.B.; Mikkili, A.M.; Bonthagorla, P.K. Critical Review on PV MPPT Techniques: Classical, Intelligent and Optimisation. *IET Renew. Power Gener.* **2020**, *14*, 1433–1452. [CrossRef]
8. Kassem, A.M. MPPT control design and performance improvements of a PV generator powered DC motor-pump system based on artificial neural networks. *Int. J. Electr. Power Energy Syst.* **2012**, *43*, 90–98. [CrossRef]
9. AI-Majidi, S.D.; Abbod, M.F.; AI-Raweshidy, H.S. A novel maximum power point tracking technique based on fuzzy logic for photovoltaic systems. *Int. J. Hydrogen Energy* **2018**, *43*, 14158–14171. [CrossRef]
10. Prabhakaran, A.; Mathew, A.S. Sliding Mode MPPT Based Control for a Solar Photovoltaic system. *Int. Res. J. Eng. Technol. (IRJET)* **2016**, *3*, 2600–2604.
11. Zang, J.H.; Wei, X.; Hu, L.; Ma, J.G. A MPPT Method based on Improved Fibonacci Search Photovoltaic Array. *Teh. Vjesn. Tech. Gaz.* **2019**, *26*, 163–170.
12. Li, H.; Peng, J.; Liu, W.; Huang, Z.; Lin, K.C. A Newton-Based Extremum Seeking MPPT Method for Photovoltaic Systems with Stochastic Perturbations. *Int. J. Photoenergy* **2014**, *2014*, 938526. [CrossRef]
13. Mazumdar, D.; Biswas, P.K.; Sain, C.; Ahmad, F.; Sarkar, R. Optimizing MPPT Control for Enhanced Efficiency in Sustainable Photovoltaic Microgrids: A DSO-Based Approach. *Int. Trans. Electr. Energy Syst.* **2024**, *2024*, 5525066. [CrossRef]
14. Atici, K.; Sefa, I.; Altin, N. Grey Wolf Optimization Based MPPT Algorithm for Solar PV System with SEPIC Converter. In Proceedings of the 4th International Conference on Power Electronics and their Applications (ICPEA) 2019, Elazig, Turkey, 25–27 September 2019; pp. 1–6.
15. Titri, S.; Larbes, C.; Toumi, K.Y.; Benatchba, K. A new MPPT controller based on the Ant colony optimization algorithm for Photovoltaic systems under partial shading conditions. *Appl. Soft Comput.* **2017**, *58*, 465–479. [CrossRef]
16. Mazumdar, D.; Biswas, P.K.; Sain, C. Performance analysis of drone squadron optimisation based MPPT controller for grid implemented PV battery system under partially shaded conditions. *Renew. Energy Focus* **2024**, *49*, 100577. [CrossRef]
17. Ahmed, J.; Salam, Z. A Maximum Power Point Tracking (MPPT) for PV system using Cuckoo Search with partial shading capability. *Appl. Energy* **2014**, *119*, 118–130. [CrossRef]
18. G. M. Abdolrasol, M.; Hannan, M.A.; Hussain, S.M.S.; Ustun, T.S.; Sarker, M.R.; Ker, P.J. Energy Management Scheduling for Microgrids in the Virtual Power Plant System Using Artificial Neural Networks. *Energies* **2021**, *14*, 6507. [CrossRef]
19. Ulutas, A.; Altas, I.H.; Onen, A. Neuro-Fuzzy-Based Model Predictive Energy Management for Grid Connected Microgrids. *Electronics* **2020**, *9*, 900. [CrossRef]
20. Barik, A.K.; Das, D.C.; Latif, A. Optimal Voltage–Frequency Regulation in Distributed Sustainable Energy-Based Hybrid Microgrids with Integrated Resource Planning. *Energies* **2021**, *14*, 2735. [CrossRef]
21. Ustun, T.S.; Hussain, S.M.S.; Ulutas, A.; Onen, A.; Roomi, M.M.; Mashima, D. Machine Learning-Based Intrusion Detection for Achieving Cybersecurity in Smart Grids Using IEC 61850 GOOSE Messages. *Symmetry* **2021**, *13*, 826. [CrossRef]
22. Ustun, T.S.; Hussain, S.M.S.; Yavuz, L.; Onen, A. Artificial Intelligence Based Intrusion Detection System for IEC 61850 Sampled Values Under Symmetric and Asymmetric Faults. *IEEE Access* **2021**, *9*, 56486–56495. [CrossRef]
23. Agarawal, P.; Bansal, H.; Gautam, A.R.; Mahela, O.M.; Khan, B. Transformer-based time series prediction of the maximum power point for solar photovoltaic cells. *Energy Sci. Eng.* **2022**, *10*, 3397–3410. [CrossRef]
24. NASA/POWER CERES/MERRA2 Native Resolution Daily Data, Dates (Month/Day/Year): 01/01/2021 Through 12/31/2021, Location: Latitude 24.8293, Longitude 93.9412. Available online: <https://power.larc.nasa.gov/data-access-viewer/> (accessed on 15 July 2024).
25. Yap, K.Y.; Sarimuthu, C.R.; Lim, J.M.Y. Artificial Intelligence Based MPPT Techniques for Solar Power System: A review. *J. Mod. Power Syst. Energy* **2020**, *8*, 1043–1059.

26. Luo, C.Y.; Ling, W.N.; Mo, D.; Mo, D.; Li, O.W.; Liang, Z.C.; Zhang, P. Power System Load Forecasting Method Based on LSTM Network. *J. Phys. Conf. Ser.* **2021**, *2005*, 012179. [[CrossRef](#)]
27. Wang, B.; Li, Y.; Yang, J. LSTM-based Quick Event Detection in Power Systems. In Proceedings of the 2020 IEEE Power & Energy Society General Meeting (PESGM), Montreal, QC, Canada, 2–6 August 2020; pp. 1–5.
28. Pattanaik, S.S.; Sahoo, A.K.; Panda, R.; Dawn, S.; Ustun, T.S. Optimal power allocation of battery energy storage system (BESS) using dense LSTM in active distribution network. *Energy Storage* **2024**, *6*, e529. [[CrossRef](#)]

**Disclaimer/Publisher’s Note:** The statements, opinions and data contained in all publications are solely those of the individual author(s) and contributor(s) and not of MDPI and/or the editor(s). MDPI and/or the editor(s) disclaim responsibility for any injury to people or property resulting from any ideas, methods, instructions or products referred to in the content.